On Chemical Reactors That Can Count

J. Gorecki,*,†,‡ K. Yoshikawa,† and Y. Igarashi†

Department of Physics, Graduate School of Science, Kyoto University and CREST, Kyoto 606-8502, Japan, and Institute of Physical Chemistry, Polish Academy of Sciences, Kasprzaka 44/52, 01-224 Warsaw, Poland

Received: April 24, 2002; In Final Form: November 7, 2002

It is known that spatially distributed excitable systems can transmit and process information if one relates the logical "true" state with a high concentration of a selected reagent and the logical "false" state with a low concentration of the same reagent. The information coded in the propagating pulses of concentration can be processed in properly arranged reactors. In this paper, we show how to build a reactor counting the number of pulses that arrive at a given point of space or that propagate within a signal channel. We discuss two types of such reactors. The first consists of many memory cells, and each of the arriving pulses excites a subsequent cell. The second gives the number of arriving pulses in the binary positional representation. All basic elements of these chemical counters have been tested experimentally using a photosensitive Ru-catalyzed Belousov−Zhabotinsky reaction.

1. Introduction

We live in a world where most information is processed electronically. The logical "true" and "false" states are represented by high and low potentials in electronic devices. However, one can also consider chemical methods of information processing.[1] In such approaches, information is coded in the concentrations of reagents. One of the methods that can be applied in chemical information processing is based on a number of enzymatic reactions proceeding in a stirred (homogeneous) reactor.[2,3] These reactions are coupled by the reagents they share. One can select the parameters describing an enzymatic reaction such that it has multiple steady states. Assigning a logical value to each of these states, we obtain a chemical device that can process information. As an alternative to a system composed of many chemically distinct reagents, one might consider a network of mass-coupled elements of a single type (for example, of bistable chemical systems[4]). Here, information is coded in patterns of states of individual nodes. Yet another approach utilizes the fact that some types of Belousov−Zhabotinsky (BZ) reactions are photosensitive. Therefore, if a spatially distributed reactor (for example, a membrane) is inhomogeneously illuminated, then the concentrations of reagents at various points are different. If the considered BZ system is in an oscillatory regime, then, when the illumination is switched off, different spatial areas start their evolution toward the limit cycle with different initial conditions. As the color of the BZ solution is related to its point on the limit cycle, one can expect that the colors of the neighboring areas (and so the contrast between them) will evolve in time. Tiny differences in illumination can be enhanced for a certain time, and in such a way, a photosensitive BZ reaction can be applied to direct image processing.[5,6]

The two methods of information processing mentioned above work in a highly parallel way. All coupled enzymatic reactions occur within the same time. The BZ reaction simultaneously proceeds in all parts of an image processing reactor. However, there are also chemical systems that behave more like "classical" sequential computers, which transform information step-by-step. Such information processing devices can be built using an excitable chemical medium. By an excitable chemical system, we mean a system involving reactions that has a single stable stationary state and the following property: small perturbations of the stationary state uniformly decay, but a large perturbation can be enhanced by orders of magnitude and evolve for a long time before it finally vanishes and the system approaches the stable state again. If a system is spatially distributed, then its local excitation can propagate in space in the form of a pulse of concentration. If we associate the state that corresponds to a high concentration of a particular reactant with the logical true state and the state corresponding to a low concentration with the logical false, then a pulse describes a bit of information traveling in space. We can process information coded in traveling pulses using properly constructed reactors. Such reactors are usually composed of regions of space in which the system is excitable and areas where some of the reactions do not occur, i.e., the system is not excitable, but reagents can diffuse through (we call such regions passive). By a clever geometrical arrangement of passive and active areas, one can construct such devices as chemical diodes[7−12] that transmit information in one direction only, logical gates,[11,13,14] chemical memory cells,[11,15] coincidence detectors,[11,16,17] that switches that change the direction of a traveling pulse.[16,17] Such systems have been studied in terms of solutions of reaction−diffusion equations for various models of reactions, and also, many of these devices have already been realized in experiments.

In this paper, we discuss reactors that can work as counters of the number of arriving pulses. They are constructed using chemical signal processing devices that have already been tested in experiments (a diode[7,10] and a memory cell[15,18]). The new signal processing element that we introduce is a T-shaped coincidence detector, which determines whether chemical signals (pulses) have met in a certain area of space. We study the response of such detectors numerically by solving the time evolution equations for concentrations within the Rovinsky−Zhabotinsky model of the ferroin-catalyzed BZ reaction,[17,19,20]

* To whom correspondence should be addressed.
† Kyoto University and CREST.
‡ Polish Academy of Sciences.

10.1021/jp021041f CCC: $25.00
Published on Web 02/15/2003

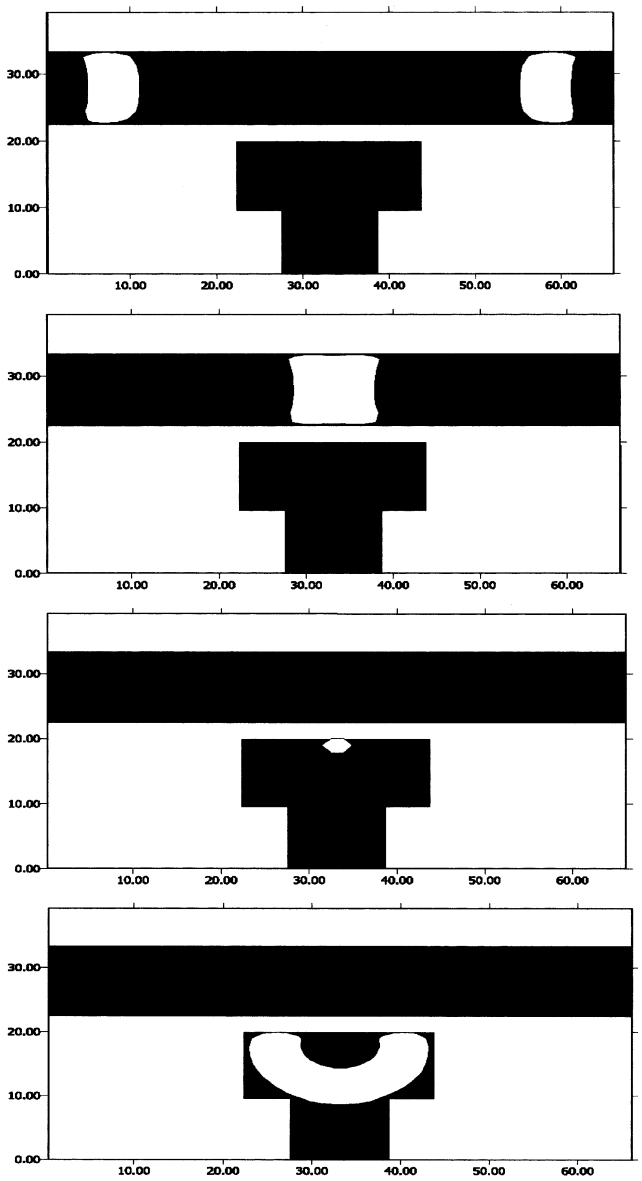

Figure 1. Time evolution of two meeting pulses in the T-shaped coincidence detector. The black color shows the distribution of the active medium; the passive areas are white. A high concentration of activator x is marked as a white contour on the active medium. Plots A−D correspond to relative times 5 (42.5 s), 15 (127.5 s), 20 (170 s), and 25 (212.5 s), respectively. The contour of concentration marks $x \geq 0.4$ in plots A, B, and D, whereas in plot C, it shows the area where $x \geq 0.01$ only.

as well as experimentally in the photosensitive Ru-catalyzed BZ system. One type of counting reactor that we considered is built of many memory cells that are sequentionally activated; thus, the activated memory cell of the highest number indicates how many pulses have arrived. The second type of counter contains a smaller number of cells, because it returns the number of arriving pulses as a binary number in a positional representation.

2. T-Shaped Coincidence Detector

The new signal processing element in our counting device is the T-shaped coincidence detector, in which the active areas form a shape similar to a T character with another horizontal bar above it (see Figure 1). In Japan, such a symbol is called yubinkyoku, and it denotes the Japanese mail. Its uppermost bar represents the signal channel in which impulses propagate. The parallel bar is the detector part. The response of such a detector can be described as follows: If a single pulse propagates in the signal channel, it does not excite the detector bar. However, if two pulses propagating in opposite directions meet in the area above the detector bar (and subsequently annihilate), the detector becomes excited, and finally an output pulse is sent through the vertical part of the T.

It is expected that such a detector should work, because it has been already shown (see Figure 1 in ref 11) that, if the width of a passive stripe separating two semiplanes of an active medium is properly selected, then a planar pulse propagating parallel to the stripe does not excite the active area on the other side of the stripe, whereas if two pulses propagating parallel in opposite directions meet they introduce an activation that can cross the barrier. This result was obtained in calculations based on a FitzHugh−Nagumo-type model of the excitable system. The detector of that point at which two waves meet that is based on this property was also discussed in ref 11. Our coincidence detector differs from the one described in ref 11, because it detects the coincidence of pulses in a region of space rather than at a point.

2.1. Numerical Simulations. Figure 1 shows the time evolution of pulses obtained in a numerical simulation of the T-shaped detector based on the Rovinsky−Zhabotinsky model. This model was proposed as a simplified description of the ferroin-catalyzed Belousov−Zhabotinsky reaction.[19,20] It is based on the well-known Field−Körös−Noyes[21,22] mechanism completed by the hydrolysis of bromomalonic acid to tartronic acid.[20] The Rovinsky−Zhabotinsky model uses two variables, x and z, corresponding to the dimensionless concentrations of the activator $HBrO_2$ and of the oxidized form of the catalyst Fe(phen)$_3^{3+}$. In the active regions that contain the catalyst, the time evolution of the concentrations of x and z is described by eqs 1 and 2

$$\frac{\partial x}{\partial \tau} = \frac{1}{\epsilon}\left[x(1-x) - \left(2q\alpha\frac{z}{1-z} + \beta\right)\frac{x-\mu}{x+\mu}\right] + \nabla_\rho^2 x \quad (1)$$

$$\frac{\partial z}{\partial \tau} = x - \alpha\frac{z}{1-z} \quad (2)$$

In the passive regions, without catalyst, the concentrations of x and z evolve according to eqs 3 and 4

$$\frac{\partial x}{\partial \tau} = -\frac{1}{\epsilon}\left[x^2 + \beta\frac{x-\mu}{x+\mu}\right] + \nabla_\rho^2 x \quad (3)$$

$$z = 0 = \text{constant} \quad (4)$$

Equations 1−4 correspond to a typical experimental situation in which the catalyst is immobilized on a membrane, whereas the activator is in the solution and can diffuse (compare refs 8 and 18). Therefore, we assume free boundary conditions between the active and passive areas.

All variables and coefficients in eqs 1−4 are dimensionless, and the real concentrations of $HBrO_2$ and Fe(phen)$_3^{3+}$ (X and Z, respectively) are related to (x and z, respectively) in the following way

$$X = \frac{k_1 A}{2k_4}x \quad (5)$$

$$Z = Cz \quad (6)$$

where $k_{\pm i}$ denotes the rate constant of the corresponding reaction in the Field−Körös−Noyes model,[19−22] $A = [HBrO_3]$, and C

$= [Fe(phen)_3^{2+}] + [Fe(phen)_3^{3+}]$. The coefficients α, β, μ, and ϵ are defined in refs 17 and 20, and they can be expressed in terms of the $k_{\pm i}$, the concentrations of reagents, and the value of the Hammett acidity function (h_0).[23−25]

In our numerical calculations for the BZ system, we use the same values of the parameters as considered in refs 19, 20, and 26: $A = 0.02$ M, $C = 0.001$ M, $k_1 = 100$ M^{-2}/s, $k_4 = 1.7 \times 10^4$ M^{-2}/s, and $q = 0.5$. The corresponding values of the scaled parameters α, β, ϵ, and μ are $0.017h_0^{-2}$, $0.0017h_0^{-1}$, 0.1176, and 0.000 51, respectively. For these values of the parameters, the system described by eqs 1 and 2 becomes excitable if $h_0 < 0.9899$.[26] As in ref 17, we have chosen $h_0 = 0.5$.

The relationships between the dimensionless time τ and distance ρ used in eqs 1−4 and the real time t and distance r are as follows

$$t = \frac{k_4 C}{k_1^2 A^2 h_0}\tau \tag{7}$$

$$r = \sqrt{\frac{k_4 C}{h_0}}\frac{1}{k_1 A}\sqrt{D_X}\rho \tag{8}$$

where D_X is the diffusion constant of the activator x. For the parameters chosen

$$t\,(\mathrm{s}) = 8.5\tau \tag{9}$$

The diffusion constant strongly depends on the medium in which the reactions proceed. In aqueous solution, it is on the order of 10^{-5} cm^2/s,[8,20,23,25,26] whereas for a reaction in a gel, it can be reduced by 2 orders of magnitude.[10] To make our results more general, we present all distances and velocities in two forms: dimensionless and as a function of the ratio of diffusion constants D_X/D_{X_0}, where the value of D_{X_0} corresponds to a particular choice of the diffusion constant: $D_{X_0} = 1 \times 10^{-5}$ cm^2/s.[20,26] The second value allows one to see more clearly the true spatial and temporal scales of the considered process because

$$r\,(\mathrm{mm}) = 9.218 \times 10^{-2}\sqrt{D_X/D_{X_0}}\rho \tag{10}$$

For the values of parameters defined above, the stationary concentrations of x and z in the active area are

$$x_{\mathrm{sa}} = 7.283 \times 10^{-4} \tag{11}$$

$$z_{\mathrm{sa}} = 1.060 \times 10^{-2} \tag{12}$$

(which is the stationary solution of eqs 1 and 2), and the stationary concentrations in the passive area (the stationary solution of eqs 3 and 4) are given by

$$x_{\mathrm{sp}} = 5.10 \times 10^{-4} \tag{13}$$

$$z_{\mathrm{sp}} \equiv 0 \tag{14}$$

In numerical calculations, we considered the T-shaped detector structure shown in black in Figure 1. The whole space is covered by a grid of 200 points in the horizontal direction and 120 points in the vertical direction. The dark stripes of the active medium are 30 grid points wide. The passive stripe separating the signal channel from the detector channel is 10 grid points wide. The distances between the grid points in both directions are the same and are equal to $\Delta\rho = 0.3301$. Therefore, in real units, the signal channel is $6\sqrt{D_X/D_{X_0}}$ (mm) long and $0.9\sqrt{D_X/D_{X_0}}$ (mm) wide; the detector part is $1.8\sqrt{D_X/D_{X_0}}$ (mm) long and also $0.9\sqrt{D_X/D_{X_0}}$ (mm) wide. Finally, the width of the passive area separating the signal channel and the detector bar is $0.3\sqrt{D_X/D_{X_0}}$ (mm) wide. No flow boundary conditions at the sides of the grid and free flow boundary conditions between the active and passive areas are used. We initiate one pulse or two pulses by locally increasing the value of x to $x_{\mathrm{ini}} = 0.1$ at one end or both ends of the signal channel.

We have performed a series of numerical calculations for the grid described above and for different values of $\Delta\rho$. They revealed that, to build a coincidence detector, one has to select the passive gap between the signal channel and the detector bar with a high precision. For the considered set of grid points, a single pulse was able to excite the signal bar for $\Delta\rho \leq 0.33$, and two meeting pulses did not excite it for $\Delta\rho \geq 0.3315$. If $0.3301 \leq \Delta\rho \leq 0.3314$ (the width of the separating passive area is such that $10\Delta\rho \in [3.301, 3.314]$), then, when just one pulse is initiated, it propagates inside the signal channel and dies at the other end. If two pulses are initiated at opposite ends of the signal channel and if they meet and annihilate above the detector bar then a pulse appears in the detector bar as shown in Figure 1A−D for $\Delta\rho = 0.3301$. The consecutive frames correspond to times $\tau = 5$, 15, 20, and 25 units (42.5, 127.5, 170, and 212.5 s, respectively). It should be also mentioned that, just after the meeting pulses annihilate, the excitation of the detector bar is very small, and the concentration of x is at the level of 0.01, whereas in a pulse it is around 0.9. Therefore, at the moment the excitation crosses the passive area, the increase in concentration of activator is almost invisible. Of course, the accuracy of ~0.4% in selecting the width of passive gap is only for the model used. It depends on the model of the excitable system and its parameters; for example, it is expected that, in the case of FitzHugh−Nagumo-type dynamics with parameters as in refs 16 and 17, the tolerance is larger.

2.2. Experimental Realization of T-Shaped Detector. We have tested whether the T-shaped coincidence detector actually works in experiments with a photosensitive BZ reaction.[28] Reactions were studied on celulose−nitrate membrane filters (A100A025A, 2.5 cm diameter, Advantec) with a pore size of 1 μm. The membrane was soaked for 3 min in the following solution of BZ reagents: 3 mL of $NaBrO_3$ (1.5 M), 1 mL of H_2SO_4 (3.0 M), 2 mL of malonic acid (1.0 M), 1 mL of KBr (0.5 M), 2.4 mL of $Ru(bpy)_3Br_2$ (8.5 mM) (all reagent-grade chemicals from Wako Pure Chemicals, Japan) and 0.6 mL of doubly distilled water. After having been soaked, the membrane was gently wiped to remove excess solution (we used a wipe tissue made by Kimwipe), placed in a Petri dish, and immediately covered with silicon oil (Shin-Etsu Chemical Co.) to prevent it from drying and to protect it from the influence of oxygen.

During the experiment, the membrane was illuminated from the bottom using the halogen bulb (JCD100V-300W) of a slide projector (Cabin, Family2) as a light source. In our experimental setup, the light intensity can be changed by the external voltage controller through which the projector is powered. The shape of the studied device is projected onto the membrane such that the active areas are dark. The experimental setup is shown in Figure 2 and it is similar to the one described in ref 29. The pulse propagation was observed under a microscope, and the image was registered by a digital video camera (Panasonic NV-DJ100), recorded by a VCR (Panasonic NV-H200G), and analyzed using standard image processing techniques. For image

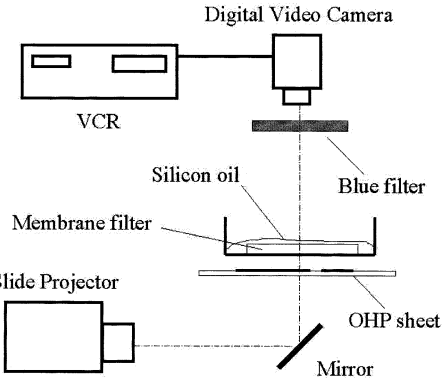

Figure 2. Experimental setup for observations of pulses in a photosensitive BZ reaction.

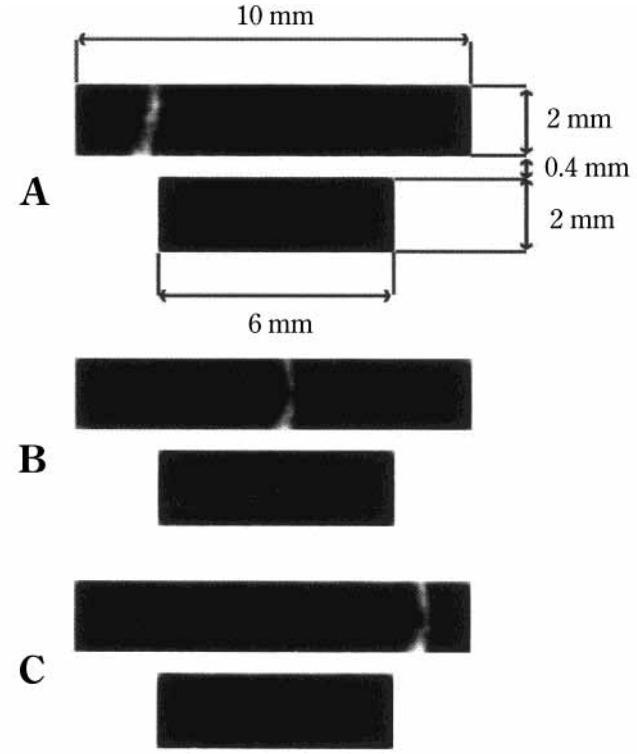

Figure 3. Time evolution of a pulse propagating from the left to the right in the experimental realization of the T-shaped coincidence detector. The black color shows the active medium; the passive areas are white. The distance between the active channel and the signal bar is 0.4 mm. A high concentration of activator is marked as a white contour on the active medium. Plots A−C correspond to times 0, 45, and 90 s, respectively.

enhancement, a blue optical filter (AsahiTechnoGlass V-42) with a maximum transparence of 410 nm was used.

In constructing the T-shaped coincidence detector, we neglected the vertical output channel to make it as simple as possible, so the coincidence detector studied in our experiments is composed of two parallel stripes only. Both stripes are 2 mm wide, the signal channel is 10 mm long, and the detector part is 6 mm long. The gap between the signal and detector channels is 0.4 mm. The light intensity was selected so that the nonilluminated parts of the membrane were excitable, whereas the excitations died in the illuminated areas. In the experiment, the light intensity was set at $I = 24$ kLx as determined by a light meter (ASONE LM-332), and the temperature was 295 ± 1 K.

Excitation pulses were initiated by gently touching the surface of the membrane with a 1-mm-thick silver wire. Figure 3 shows

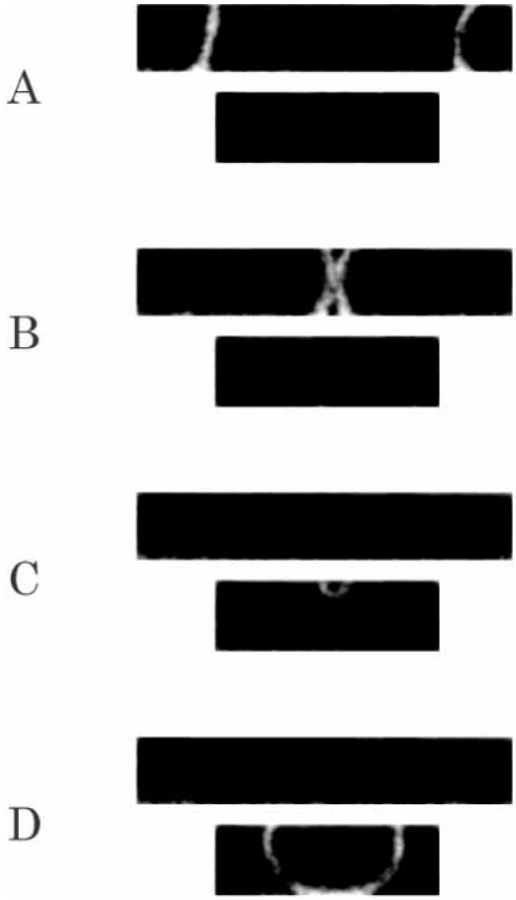

Figure 4. Time evolution of two pulses that meet in the signal channel of the experimental realization of the T-shaped coincidence detector. The black color shows the active medium; the passive areas are white. The distance between the active channel and the signal bar is 0.4 mm. A high concentration of activator is marked as a white contour on the active medium. Images A−D correspond to times 0, 40, 60, and 80 s, respectively.

the evolution of the system when the pulse is initiated at left site of the signal channel only. The consecutive pictures (Figure 3A−C) show the positions of the pulse of excitation at $t = 0$, 45, and 90 s. It is clear that nothing interesting happens: the pulse of excitation propagates along the signal channel, does not escape, and dies at the other end. The time evolution in the case where two excitations at both ends of the signal channel are introduced is shown in Figure 4. Here, the consecutive frames (A−D) correspond to times $t = 0$, 40, 60, and 80 s. At the beginning, the initiated pulses propagate in opposite directions (Figure 4A). They collide (Figure 4B) and later annihilate. For a few seconds, no trace of pulses is seen in the signal channel. Next, a small excitation in the detector channel appears (Figure 4C). Finally, this excitation expands, and a new pulse of excitation propagates inside the detector channel (Figure 4D). This experiment was repeated a few times to ensure that such coincidence detection works for different positions of the point at which the pulses meet. The results presented in Figure 4 are in a perfect qualitative agreement with the calculations based on the Rovinsky−Zhabotinsky model (Figure 1). They support our statement that the proposed geometry of the T-shaped coincidence detector can be used for various excitable chemical systems. In the experiment, as in the calculations, the proper choice of the distance between the signal channel and the detector bar was the most important and difficult. There is no reason to make a quantitative comparison between the results of calculations and the experiment because the Rovinsky−

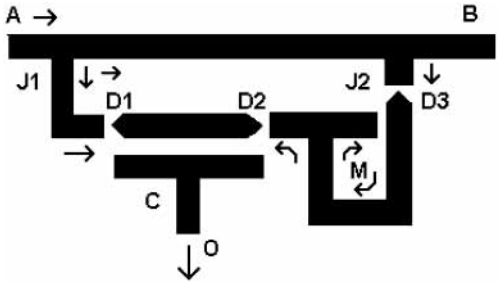

Figure 5. Scheme of basic counting element. The active parts are black; the passive areas are white. The counting element is composed of a T-shaped coincidence detector C; a memory cell M; and three diode junctions D1, D2, and D3. The arrows show the direction in which the pulses propagate.

Zhabotinsky model describes another type of BZ reaction. Nevertheless, the calculated distance between the signal channel and the detector bar gives a reasonable estimation of the width used in the experiment.

3. Counting Reactors

In this section, we describe how to build a counting chemical reactor using such elements as a chemical signal diode, a memory cell, and a T-shaped coincidence detector. The scheme of a basic counting element is shown in Figure 5. The active areas are black, and the passive areas are white. One can easily recognize a T-shaped coincidence detector (C), a memory ring (M), and three diodes (D1−D3). Let us assume that a pulse of excitation appears at point A and propagates along the upper signal channel toward B as the arrow shows. It splits at the first junction J1. One of the pulses enters the signal channel of coincidence detector C and dies at diode D2. Its second part propagates in the signal channel toward point B and then separates again at the second junction J2. The pulse propagates through diode D3 and activates memory device M, initiating a circulating pulse inside it. The barrier separating the vertical and horizontal channels in the memory device is impenetrable for a signal propagating from D3, so the pulse is forced to rotate clockwise.[15] Diode D3 is important, because, without it, the pulses from the memory device could enter the signal channel again and interfere with the incoming pulses. The pulse circulating in the memory separates at the T junction and enters the coincidence detector through diode D2. Therefore, after the first pulse has arrived, coincidence detector C is regularly loaded with the pulses from the memory device. These pulses die at diode D1 and do not interfere with the signal channel. Now, if a second pulse appears in signal channel AB, it enters coincidence detector C and meets the pulse from the memory there. As a consequence, the detector bar becomes excited, and it sends a pulse through channel O, as the arrow shows. Thus, a pulse in output O indicates that two pulses propagated in the considered signal channel AB.

Now, it is easy to build a counting reactor. Let us consider the structure shown in Figure 6. Here, one can recognize two basic counting elements presented in Figure 5. The memory cell of the first one (M1) is loaded directly from the signal channel; the memory cell of the second counting element (M2) is loaded from the output (O1) of the first coincidence detector C1. If memory cell M2 is not loaded, no coincidence is detected at C2, so there is no signal in output channel O2. M2 is loaded by the signal from O1, and this signal appears only after the second pulse has propagated in the signal channel AB. Therefore, coincidence detector C2 sends its first pulse into output channel O2 only after the third pulse has propagated in

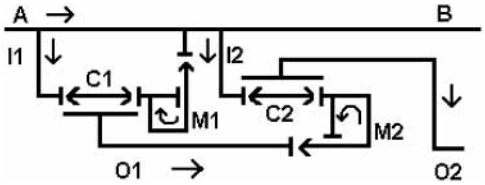

Figure 6. Scheme of a counting chemical reactor. The consecutive memory cells (M1, M2, ...) are loaded one-by-one as the new pulses appear in the signal channel AB. The arrows show the direction in which the pulses propagate.

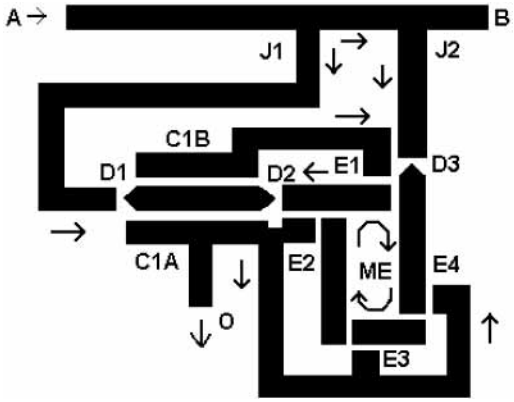

Figure 7. Scheme of a modulo 2 counting element. The active parts are black; the passive areas are white. The counting element is composed of an eraseable memory cell ME; three diode junctions D1, D2, and D3; and a double coincidence detector (C1A, C1B) that is linked to output channel O, as well as to four memory erasing channels E1−E4. The arrows show the direction in which the pulses propagate.

channel AB. We can use this pulse to load yet another memory device linked with another coincidence detector in a similar way as C2 and M2. This additional counting element produces its first output pulse after the fourth pulse in the AB channel. If one extends the structure by a number of counting elements then the loaded memory device of the highest number gives the number of pulses that propagated. In this device, the states of the memory devices that were loaded earlier are completely irrelevant.

However, the counting reactor presented above requires a large structure composed of many memory cells and coincidence detectors. We can reduce their number if we use a memory cell that can be both written and erased.[15] The structure of a basic counting element based on such a memory cell is shown in Figure 7. Its design is similar to that presented in Figure 5, but it contains two significant modifications. First, the memory is designed such that it can be erased by a signal from the coincidence detector. The memory ring shown is built of four separate parallelogram-shaped active areas. The gaps are selected such that a pulse can propagate clockwise but not anticlockwise, because in the second case, it propagates parallel to the gaps and thus is not able to cross them. The memory ring is surrounded by erasing channels that are connected with two coincidence detectors C1A and C1B. Erasing signals enter the memory ring from gates E1−E4, meet the pulse rotating in the memory, and annihilate with it. The erasing pulses that have not met the memory pulse on their way die at the nearest gap. In this respect, the number of four parts is not at all critical, and the memory cell can be composed of a larger number of pieces provided that the signal that loads memory is introduced in a direction that creates a stable rotating pulse and that the number of erasing signals are introduced such, that the signals die after some time. As in the counting device shown in Figure 5, the first pulse separates at junctions J1 and J2, the pulse

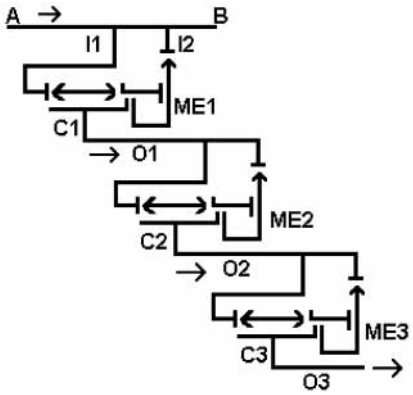

Figure 8. Scheme of a counting chemical reactor that gives the number of pulses as a positional binary number. The consecutive memory cells (ME*i*) are loaded and erased by modulo 2^i chemical pulses. The arrows show the direction in which the pulses propagate.

propagating down at J1 dies at diode D2, and the pulse propagating down J2 loads the memory cell. When the second pulse comes, it meets a signal from the memory at the coincidence detector, which becomes active and sends a pulse into output channel O, as well as to the erasing gates. Note that J1 is shifted toward J2 if compared with Figure 5. If the second pulse activates the coincidence detector and sends erasing signals too early, then its part propagating along J2 might find the memory ring empty and load it. If junctions J1 and J2 are close to each other, then the second pulse interacts with the memory first and next arrives at the coincidence detector. Even if it loads into the memory cell, the cell will be cleared by the erasing signals. Therefore, the structure shown in Figure 7 works such that, after every odd pulse, the memory ring is loaded and, after every even pulse, the memory ring is deactivated and a pulse is sent into the output channel. Such a structure represents a modulo 2 counter.

We can link many of such counters, forming the structure shown in Figure 8. For simplicity, we have not drawn all erasing channels here. The signal from output channel O1 loads counter C2, ME2, which produces a modulo 4 signal in channel C2 (i.e., one pulse after every four pulses that propagate in channel AB). This signal loads the counter C3, ME3, and the output in O3 is a modulo 8 signal, and so on. If we assign values of 1 to the active state of memory and 0 to the passive state, then the number of propagating pulses N is equal to

$$N = \mathrm{ME0} + 2 \times \mathrm{ME1} + 4 \times \mathrm{ME2} + \ldots \qquad (15)$$

because the consecutive memory devices give the digits of the number of pulses in the positional binary representation.

4. Conclusions

In this paper, we have discussed how one can build a reactor that contains information on the number of pulses of excitation that have propagated inside a given signal channel. The structures of our counting reactors are quite general, so they can be applied to other spatially distributed excitable systems in which the pulses of excitation carry information. Moreover, they can be used as time devices that send a signal after an assumed number of pulses arrived to the system.

All elements of our counting reactors were tested independently in experiments with BZ-type reactions, so we believe they should work. However, the spatial scale of the counting device is too large to be studied in the available experimental facilities. In our experimental setup for a photosensitive BZ reaction shown in Figure 2, the light intensity is uniform at distances smaller than 10 mm from the center, and any of the basic counting units (Figures 5 and 7) is too large to fit in. We believe that it might be easier to build a counting reactor using a membrane with a catalyst introduced by lithography, as was done in ref 30.

Of course, our counting structures are not perfectly free of mistakes. One can expect a malfunction of the coincidence detector if the signal from the memory and an incoming pulse meet in the diode area. However, if we double the coincidence detector and the memory device on the other site of the signal channel such that the signals from memory arrive to detectors at different times and then combine signals by an OR gate, then the structure will be more reliable. The discussion presented above applies to the case where the frequency of pulses in the signal channel AB is low. If the frequency is high, then the discussed structures might exhibit very complex behavior, as pointed out in ref 31.

Acknowledgment. The authors are grateful to Mr. T. Ichino for technical assistance. The present study is partially supported by a Grant-in-Aid from the Ministry of Education, Culture, Sports, Science and Technology of Japan.

References and Notes

(1) Maselko, J. *Mater. Sci.* **1995**, *5*, 155.
(2) Okamoto, M.; Maki, Y.; Sekiguchi, T.; Yoshida, S. *Physica D* **1995**, *84*, 194 and references therein.
(3) Arkin, A.; Ross J. *Biophys. J.* **1994**, *67*, 560.
(4) Hjelmfelt, A.; Ross, J. *Physica D* **1995**, *84*, 180. See also: Hjelmfelt, A.; Ross, J. *J. Phys. Chem.* **1993**, *97*, 7988. Hjelmfelt, A.; Schneider, F. W.; Ross, J. *Science* **1993**, *260*, 335.
(5) Kuhnert, L.; Agladze, K. I.; Krinsky, V. I. *Nature* **1989**, *337*, 244.
(6) Rambidi, N. G.; Maximychev, A. V. *BioSystems* **1997**, *41*, 195.
(7) Agladze, K.; Aliev, R. R.; Yamaguchi, T.; Yoshikawa, K. *J. Phys. Chem.* **1996**, *100*, 13895.
(8) Kusumi, T.; Yamaguchi, T.; Aliev, R. R.; Amemiya, T.; Ohmori, T.; Hashimoto, H.; Yoshikawa, K. *Chem. Phys. Lett.* **1997**, *271*, 355.
(9) Yoshikawa, K.; Motoike, I. N.; Kajiya, K. *IEICE Trans. Electron.* **1997**, *E80-C*, 931.
(10) Yamaguchi, T.; Kusumi, T.; Aliev, R. R.; Amemiya, T.; Ohmori, T.; Nakaiwa, M.; Urabe, K.; Kinugasa, S.; Hashimoto, H.; Yoshikawa, K. *ACH−Models Chem.* **1998**, *135*, 401.
(11) Motoike, I. N.; Yoshikawa, K. *Phys. Rev. E* **1999**, *59*, 5354.
(12) Toth, A.; Horvath, D.; Yoshikawa, K. *Chem. Phys. Lett.* **2001**, *345*, 471.
(13) Toth, A.; Showalter, K. *J. Chem. Phys.* **1995**, *103*, 2058.
(14) Steinbock, O.; Kettunen, P.; Showalter, K. *J. Phys. Chem.* **1996**, *100*, 18970.
(15) Motoike, I. N.; Yoshikawa, K.; Iguchi, Y.; Nakata, S. *Phys. Rev. E* **2001**, *63*, 036220.
(16) Sielewiesiuk, J.; Gorecki, J. *Acta Phys. Pol. B* **2001**, *32*, 1589.
(17) Sielewiesiuk, J.; Gorecki, J. *J. Phys. Chem. A* **2001**, *105*, 8189.
(18) Lazar, A.; Noszticzius, Z.; Försterling, H.-D.; Nagy-Ungvarai, Z. *Physica D* **1995**, *84*, 112.
(19) Rovinsky, A. B.; Zhabotinsky, A. M. *J. Phys. Chem.* **1984**, *88*, 6081.
(20) Rovinsky, A. B. *J. Phys. Chem.* **1986**, *90*, 217.
(21) Field, R. J.; Körös, E.; Noyes, R. M. *J. Am. Chem. Soc.* **1972**, *94*, 8649.
(22) Scott, S. K. *Oscillations, Waves and Chaos in Chemical Kinetics*; Oxford University Press: Oxford, U.K., 1994; pp 27−29.
(23) Zhabotinsky, A. M.; Buchholtz, F.; Kiyatkin, A. B.; Epstein, I. R. *J. Phys. Chem.* **1993**, *97*, 7578.
(24) Hammett, L. P. *Physical Organic Chemistry. Reaction Rates, Equilibria and Mechanisms*; McGraw-Hill: New York, 1970.
(25) Aliev, R. R.; Rovinsky, A. B. *J. Phys. Chem.* **1992**, *96*, 732.
(26) Frankowicz, M.; Kawczyński, A. L.; Gorecki, J. *J. Phys. Chem.* **1991**, *95*, 1265.
(27) Miyakawa, K.; Sakamoto, F.; Yoshida, R.; Kokufuta, E.; Yamaguchi, T. *Phys. Rev. E* **2000**, *62*, 793.
(28) Kadar, S.; Wang, J.; Showalter, K. *Nature* **1998**, *391*, 770.
(29) Agladze, K.; Toth, A.; Ichino, T.; Yoshikawa, K. *J. Phys. Chem. A* **2000**, *104*, 6677.
(30) Suzuki, K.; Yoshinobu, T.; Iwasaki, H. *Jpn. J. Appl. Phys. 2* **1999**, *38*, L345. Suzuki, K.; Yoshinobu, T.; Iwasaki, H. *J. Phys. Chem. A* **2000**, *104*, 6602.
(31) Sielewiesiuk, J.; Gorecki, J. *Phys. Chem. Chem. Phys.* **2002**, *4*, 1326.